PCCP
Physical Chemistry Chemical Physics

Accepted Manuscript

This article can be cited before page numbers have been issued, to do this please use: B. Feng, E. Sundin, P. Lincoln and A. K. F. Mårtensson, *Phys. Chem. Chem. Phys.*, 2020, DOI: 10.1039/D0CP00845A.

ROYAL SOCIETY OF CHEMISTRY

rsc.li/pccp

View Article Online
DOI: 10.1039/D0CP00845A

ARTICLE

DNA threading intercalation of enantiopure $[Ru(phen)_2bidppz]^{2+}$ induced by hydrophobic catalysis

Received 00th January 20xx,
Accepted 00th January 20xx

DOI: 10.1039/x0xx00000x

Bobo Feng[a], Elin Sundin[a], Per Lincoln[a] and Anna K. F. Mårtensson[a,b]*

The enantiomers of a novel mononuclear ruthenium(II) complex $[Ru(phen)_2bidppz]^{2+}$ with an elongated dppz moiety were synthesized. Surprisingly, the complex showed no DNA intercalating capability in an aqueous environment. However, by the addition of the water-miscible polyethylene glycol ether PEG-400, the self-aggregation of the hydrophobic ruthenium(II) complexes was counter-acted, thus strongly promoting the DNA intercalation binding mode. This mild alteration of the environment surrounding the DNA polymer does not damage or alter the DNA structure but instead enables more efficient binding characterization studies of potential DNA binding drugs.

Introduction

The molecular mechanisms behind the DNA interactions of ruthenium(II) polypyridyl complexes have long since attracted interest due to their potential use in DNA-targeting pharmacotherapies.[1] Particular attention has been given to the so-called light-switch complexes $[Ru(bpy)_2dppz]^{2+}$ and $[Ru(phen)_2dppz]^{2+}$ (bpy = 2,2'-bipyridine; phen = 1,10-phenanthroline; dppz = dipyrido[3,2-*a*:2',3'-*c*]phenazine) which, upon intercalation of the dppz moiety between the base pairs, display an intense luminescence.[2] While most mononuclear Ru(II) dppz complexes readily intercalate to DNA with low sequence specificity, binuclear Ru(II) complexes show in general both greater selectivity and binding affinity due to increased size and charge, respectively.[3] The semi-rigid binuclear complex $[\mu\text{-bidppz}[phen)_4Ru_2]^{4+}$ (**Ru-2**, see Scheme 1; bidppz = 11,11'-bi(dipyrido[3,2-*a*:2'3-*c*]phenazinyl has been shown to bind to DNA by having one of its bulky Ru(II) centres passed through the base pair stack, an unusual binding mode called threading intercalation which requires a transient large conformational change to occur in the DNA structure.[4] With calf thymus DNA, the binding requires several hours to reach completion, even at high ionic strength and elevated temperature. As the impact of effective association rates has gained more and more attention as a way to increase *in vivo* target occupancy or to reduce undesired side effects[5], it is desirable to improve the extremely slow association rate of **Ru-2** while retaining its strong binding affinity to DNA. For the mononuclear complex $[Ru(phen)_2bidppz]^{2+}$ (**Ru-1**, see Scheme 1) we expected an accelerated association rate since it is formally obtained from **Ru-2** by removing one of the bulky Ru(II) centres. While there are a few previous reports published on the synthesis and characterization of racemic **Ru-1**, the focus has mainly been on electrochemical and photophysical properties rather than DNA binding capability.[6] In addition, the chiral nature of these octahedral complexes greatly affects their interactions with DNA, another chiral molecule. The importance of these diastereomeric effects have previously been demonstrated by our group[7], motivating us to synthesize **Ru-1** into its right-handed (Δ) and left-handed (Λ) form for this study. Surprisingly, in pure buffer, we found no evidence for DNA intercalation of neither enantiomer of **Ru-1**: no emission intensity increase and only very weak linear dichroism could be observed, even after several days at 50°C.

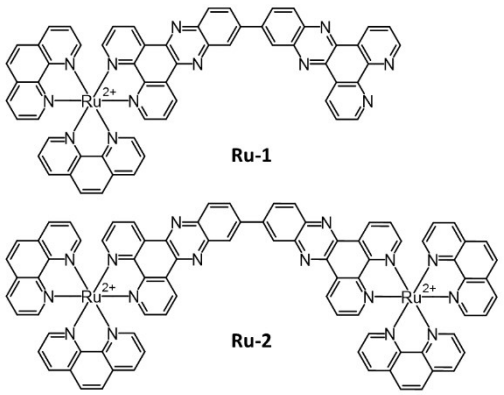

Scheme 1. Structures of $[Ru(phen)_2bidppz]^{2+}$ (**Ru-1**) and $[\mu\text{-bidppz}(phen)_4Ru_2]^{4+}$ (**Ru-2**).

Water-miscible hydrophobic co-solutes can reduce the base stacking energy and enable longitudinal breathing of the DNA polymer in aqueous solution, resulting in the appearance of transient holes in the base pair stack without affecting the overall B-DNA conformation. As recently demonstrated by Feng

[a]*Department of Chemistry and Chemical Engineering, Kemigården 4, SE-412 96 Gothenburg, Sweden.*
[b]*Wallenberg Laboratory for Cardiovascular and Metabolic Research, Institute of Medicine, University of Gothenburg, Sahlgrenska University Hospital, Bruna Stråket 16, SE-413 45 Gothenburg, Sweden.*
E-mail: anna.martensson@wlab.gu.se
Electronic Supplementary Information (ESI) available: See DOI: 10.1039/x0xx00000x

View Article Online
DOI: 10.1039/D0CP06815A

et al.[8] a significantly accelerated threading intercalation of **Ru-2** into DNA is observed in the presence of ethylene glycol ethers.

Interestingly, a slow increase of emission intensity is observed following addition of the polyethylene glycol ether PEG-400 to an aqueous solution of **Ru-1** in the presence of DNA at 50°C. In the present work we have used flow linear dichroism, association kinetics (measured as emission intensity) and emission lifetimes to characterize the mode of DNA interaction in aqueous PEG-400 of both **Ru-1** enantiomers and, for comparison, the well-established thread-intercalator **Ru-2**.

Experimental

Materials

All experiments were performed in aqueous buffer solution (pH = 7.0) containing 50 mM NaCl and 1 mM cacodylate (dimethylarsinic acid sodium salt). Stock solutions of calf thymus DNA (ctDNA) (~5 mM nucleotides) were prepared by dissolving highly polymerized type I sodium salt calf thymus DNA (Sigma-Aldrich) in 150 mM NaCl buffer solution. The solution was filtered two times through a 0.7 µm polycarbonate filter and diluted with 50 mM NaCl buffer solution to appropriate concentration. Stock solutions of the complexes (~1 mM) were prepared by dissolving the chloride salts in 50 mM NaCl buffer solution. Concentrations were determined spectrophotometrically using extinction coefficients: $\varepsilon_{258\ nm}$ = 6600 M^{-1} cm^{-1} per nucleotide for ctDNA, $\varepsilon_{412\ nm}$ = 30 900 M^{-1} cm^{-1} for [Ru(phen)$_2$bidppz]Cl$_2$ (**Ru-1**) and $\varepsilon_{408\ nm}$ = 75 800 M^{-1} cm^{-1} for [µ-bidppz(phen)$_4$Ru$_2$]Cl$_4$ (**Ru-2**). Polyethylene glycol (PEG) 400 (polydisperse, average MW = 400, Rectapur, VWR) was added directly to the samples. Solid NaCl (≥ 99.5%, Sigma-Aldrich) was weighed on an analytical balance (Sartorius MSE225S) and added in the last step of sample preparation to avoid being diluted by the addition of PEG-400.

Sample preparation

Δ-[Ru(phen)$_2$pq](arsenyl-D(-)-tartrate)$_2$, Λ-[Ru(phen)$_2$pq](arsenyl-L(+)-tartrate)$_2$ (pq = 1,10-phenanthroline-5,6-dione) and [µ-bidppz(phen)$_4$Ru$_2$]Cl$_4$ (**Ru-2**) enantiomers were prepared as previously reported.[9]

The synthetic route for preparation of [Ru(phen)$_2$bidppz]Cl$_2$ (**Ru-1**) is shown in Scheme 2.

General information about the syntheses. 3,3'-Diaminobenzidine, sodium acetate trihydrate, tetra-*n*-butylammonium chloride and ammonium hexafluorophosphate were purchased from Sigma-Aldrich and used as received without further purification. ^{1}H NMR spectra were recorded on a Varian UNITY-VXR 5000 (400 MHz) spectrometer and chemical shifts are reported with acetone-d_6 (δ_H = 2.05 ppm) as reference.

Synthesis of ligand. 4-Dipyrido[3,2-*a*:2',3-*c*]phenazine-11-yl-1,2-benzenediammonium chloride (1). 0.22 g (1.0 mmol) of 3,3'-Diaminobenzidine (DAB) was dissolved in a mixture of 10 mL EtOH, 10 mL H_2O and 1 mL HOAc. 0.381 g of NaOAc · 3H_2O was dissolved in 5 mL H_2O. 0.105 g (0.5 mmol) of 1,10-Phenanthroline-5,6-dione (pq) was dissolved in 10 mL heated EtOH. The solutions of DAB and NaOAc were mixed together, followed by the slow adding of the pq solution in small aliquots to the stirred mixture. A red-precipitate formed, which was collected on a filter and washed with a mixture of 10 mL EtOH, 10 mL H2O and 1 mL HOAc. The red-brown powder (0.196 g after drying) was dissolved in 20 mL of 0.1 M HCl and the solution was heated. The heated solution was filtered, the filter washed with warm 0.1 M HCl, and the combined filtrates then evaporated under reduced pressure in a water bath for ~30 minutes to give the solid product **1** as red-brown, shiny, flat crystals (0.169 g, 0.42 mmol, 84% yield calculated from the starting material pq).

Synthesis of ruthenium complexes. Δ- and Λ-[µ-bidppz(phen)$_2$Ru]Cl$_2$ (Ru-1). 0.20 g of Λ-[Ru(phen)$_2$pq]arsenyl-L(+)-tartrate)$_2$ (phen = 1,10-phenanthroline; pq = 1,10-phenanthroline-5,6-dione) and 0.096 g of **1** were dissolved in two separate solutions of 4 mL of 50% HoAc (aq) while heated in a water bath. While keeping the dissolved Λ-[Ru(phen)$_2$pq]$^{2+}$ warm, **1** was added in small aliquots resulting in a bright red-orange solution. After cooling, the product was precipitated using NH_4PH_6 dissolved in water, collected on a filter and washed with EtOH followed by diethyl ether. Purification of Λ-[Ru(phen)$_2$bidppz](PF$_6$)$_2$ dissolved in CH_3CN was done using column chromatography with EtOH/CH_3CN (1 : 4) and neutral Al_2O_3. The eluate containing the pure orange product was collected and reduced to ~1 mL by evaporating with a stream of N_2 under mild heating. About 0.5 g of ([$CH_3(CH_2)_3$]$_4$NCl), dissolved in 1 mL of acetone, was added in increasing portions while stirring until the solution was only weakly yellow and the precipitation complete. The red precipitation was left overnight and collected on a filter the following day. The product was washed with acetone followed by diethyl ether to yield Λ-[Ru(phen)$_2$bidppz]Cl$_2$ as a red powder (0.16 g, 0.15 mmol, 67%, yield calculated from the starting material, [Ru(phen)$_2$pq](arsenyl-L(+)-tartrate)$_2$) The procedure was repeated with Δ-[Ru(phen)$_2$pq](arsenyl-D(-)-tartrate)$_2$ to yield the opposite enantiomer Δ-[Ru(phen)$_2$bidppz]Cl$_2$ (0.13 g, 0.12 mmol, 56%). UV/vis (in water; λ_{max} in nm, $\varepsilon/10^3$ M^{-1} cm^{-1} enclosed in parenthesis): 412 (30.9), 304 (53.8) 263 (81.3), 221 (66.9), 204 (63.5). ^{1}H NMR (as PF_6 salt, 400 MHz, acetone-d_6): δ (ppm) = 9.32 (d, 1H, J = 8.0 Hz), 9.24 (d, 1H, J = 8.0 Hz), 8.85 (d, 1H, J = 8.0 Hz), 8.80 (t, 1H, J = 8.0 Hz), 8.59-8.52 (m, 4H), 8.41 (s, 1H), 8.28-8.14 (m, 8H), 8.09-7.92 (m, 8H), 7.79 (d, 1H, J = 8.0 Hz), 7.74-7.71 (dd, 1H), 7.66 (m, 1H), 7.57-7.53 (m, 3H), 7.47-7.45 (m, 2H), 7.40-7.35 (dd, 1H). UV/vis absorption and NMR measurements were in accordance with previous reports and showed no significant impurities. Extensive characterization of **Ru-1** and structurally similar complexes have already been published elsewhere.[6]

Instrumentation

Absorption spectra were recorded on a Varian Cary 4000 UV/vis spectrophotometer with buffer as baseline using a 1 cm quartz

View Article Online
DOI: 10.1039/D0CP00845A

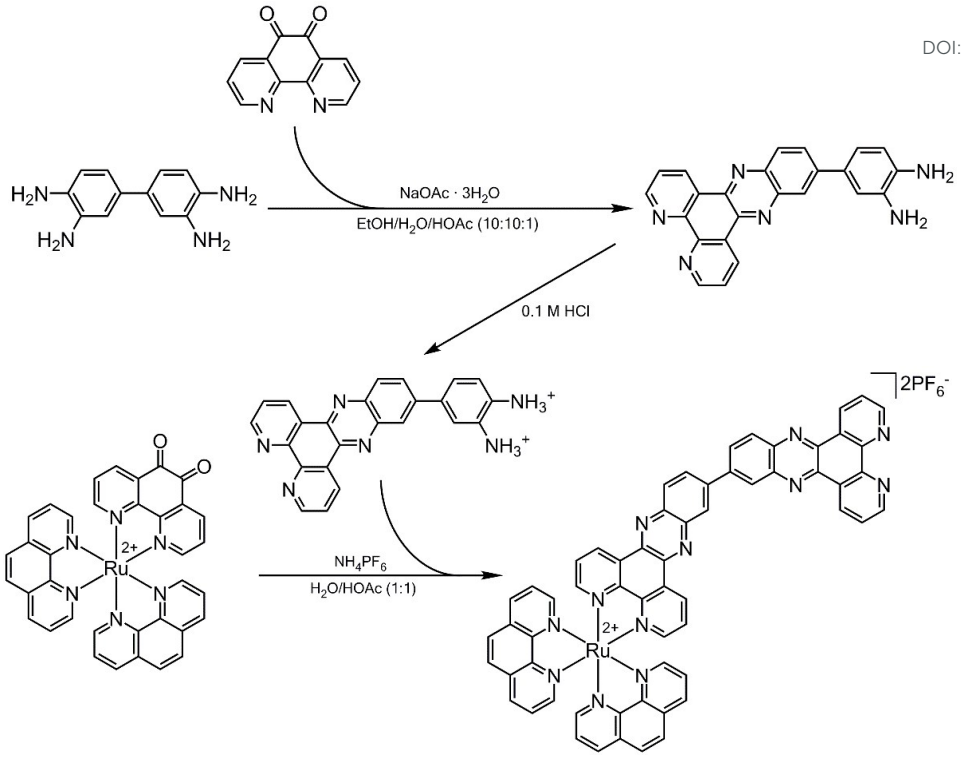

Scheme 2. Synthesis route for **Ru-1**.

cell. Linear dichroism (LD) was measured on a Chirascan LD spectropolarimeter on samples oriented in an outer-rotating Couette flow cell with a 1 mm path length at a rate of 480 rpm. Spectra were corrected for baseline contributions by subtraction of the corresponding spectra recorded without rotation. Circular dichroism (CD) spectra were recorded on a Chirascan CD spectropolarimeter with buffer as baseline using a 1 cm quartz cell. In general, 5 CD spectra were averaged for each sample. Emission spectra were recorded on a Varian Cary Eclipse Fluorescence spectrophotometer using a 1 cm quartz cell. The samples were excited at 410 nm and emissions were recorded at 500-800 nm (10 nm excitation slit, 5 nm emission slit and 700 V photomultiplier voltage).

Binding kinetics were studied using a Varian Cary Eclipse Fluorescence spectrophotometer equipped with a multicell temperature controller using a 1 cm quartz cell at 50°C under magnetic stirring. The samples were excited at 410 nm, and the change in emission intensity was studied at 620 nm (0.2-0.4 s averaging time, 10 nm excitation slit, 5 nm emission slit and 700 V photomultiplier voltage).

Excited state lifetimes were measured using time correlated single photon counting, a 405 nm diode (PicoQuant) with 250 kHz repetition rate was used as excitation source and an MCP-PMT (1024 channels, 10 000 counts in the peak channel) was used as detector. The decays were fitted by deconvolution with the instrument response function to biexponential decays.

For the qualitative and comparative evaluation of the self-aggregation of **Ru-1** and **Ru-2**, absorption spectra of the Δ-enantiomers of the two complexes were recorded in different solvents. The solvents used were a MeOH/H_2O (1:1) mixture, MilliQ-pure water, 50 mM NaCl buffer, 50 mM NaCl buffer with added 15% PEG-400 or 40% PEG-400 (w/w). A small volume (10 µL) of complex stock solution (**Ru-1**: 1 mM; **Ru-2**: 0.4 mM, in water) was added to each solvent directly into the 1 cm quartz cell. All measurements were performed in triplicates to ensure reproducibility.

Data analysis

Kinetic traces of DNA association were fitted using the curve fitting tool in the Matlab software package (Mathworks, Inc.). The reaction yield was calculated by normalizing the observed fluorescence with respect to the final intensity when no further reaction was observed. Two exponentials were needed to fit the kinetic data for all samples.

The kinetic traces for DNA association were fitted using a bi-exponential model:

$$Y(t) = 1 - \alpha_1 e^{-k_1 t} - (1 - \alpha_1) e^{-k_2 t} \quad (1)$$

where α_1 is the fraction of the fast rate constant, k_1 is the fast rate constant and k_2 is the slow rate constant.

Results and discussion

The high enantiomeric purity of the newly synthesized and resolved **Ru-1** complex was confirmed by circular dichroism (CD) (shown in Fig. S2 in ESI). Similar to the corresponding enantiomers of binuclear complex **Ru-2**, we observed a strong signal at ~270 nm originating from the phen ligand exciton.

Fig. 1 shows the absorption spectra of Δ-**Ru-1**, free as well as in the presence of calf thymus DNA (ctDNA), in buffer

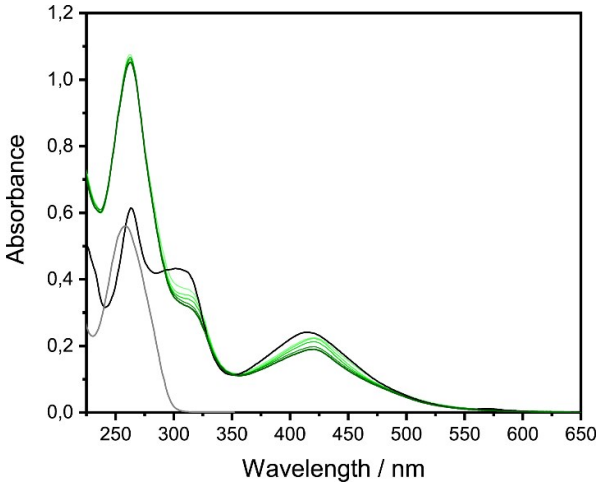

Figure 1. Absorption spectra of Δ-**Ru-1** in the presence of ctDNA at [base pairs]/[complex] ratio 5 in 50 mM NaCl aqueous buffer solution with 20% (w/w) PEG-400. The color change from light to dark specify spectral change with time (0, 0.5, 1.5, 24 and 48 h; green) after 50°C incubation. The black line shows the complex without the addition of ctDNA. The gray line shows ctDNA alone. The concentration of ctDNA is 80 μM nucleotides.

containing 20% (w/w) PEG-400 after different incubation times at 50°C. A significant hypochromic change with time, accompanied by a small red shift, is observed in the strong bidppz π→π* intraligand transition (IL) absorption band at 310 nm. The same is observed for the peak at 410 nm, there the bidppz π→π* transition overlaps with a broad band of metal to ligand charge transfer (MLCT) transitions (centred at 440 nm for the parent $[Ru(phen)_2dppz]^{2+}$ complex).[9a] The spectral changes are similar for those observed for the slow threading intercalative binding of the binuclear analogue **Ru-2** in pure buffer[3a,3c] and are suggestive of an intercalative binding mode for the bidppz ligand.[9a,10] Similar, albeit not as pronounced, hypochromic effects were observed for the Λ-enantiomer (shown in Fig. S1 in ESI). By contrast, in the absence of PEG-400, only a slight red-shift and very weak hypochromicity is observed, even after several days incubation at 50°C.

Linear dichroism (LD) measures the difference in absorption between polarized light parallel and perpendicular to a macroscopic orientation axis (*e.g.* the DNA helix axis in flow-oriented DNA), making it possible to investigate the binding geometry of small chromophores bound to DNA.[11] Fig. 2 shows the flow LD spectra of Δ-**Ru-1** in the presence of ctDNA and 20% PEG-400 recorded at ambient temperature after different times of incubation at 50°C. Before incubation, the LD spectrum shows essentially only the DNA signal, indicating that the initial interaction with DNA does not result in a distinct orientation of the complex. During the progress of several days, strong LD bands appear in the visible region. The similarities to the LD spectrum of threaded ΔΔ-**Ru-2** (Fig. 2, dotted black line, obtained after incubation of the complex with DNA in buffer with 20% PEG-400 at 50°C for 24 hours) indicate that the binding geometry and binding mode of **Ru-1** is similar despite the lack of one bulky Ru centre. As can be observed after 7 days incubation, the LD band at 270 nm, has changed from being initially negative to positive. The LD bands in the visible region, in contrast, appears unchanged past 2 days. Interestingly, by subtracting the LD signal after 2 days with the signal after 7 days (LD_{2d}-LD_{7d}), the remaining LD spectrum appears identical to a pure DNA signal (Fig. 2, inset), indicating a slow process affecting the orientation of the DNA polymer without much effect on the geometric orientation of the threaded bridging ligand of Δ-**Ru-1**. The LD spectra of Λ-**Ru-1** (Fig. S3, ESI) showed a similar slow geometrical rearrangement towards an intercalated binding mode.

The reduced LD (LD^r), which is the LD divided by the isotropic absorbance, is very similar for ΔΔ-**Ru-2** at both 0% and 20% PEG-400, indicating little or no change in the geometric orientation in the presence of PEG-400 (Fig. 3). In contrast, the shape of the LD^r spectra for Δ-**Ru-1** changes dramatically from an almost

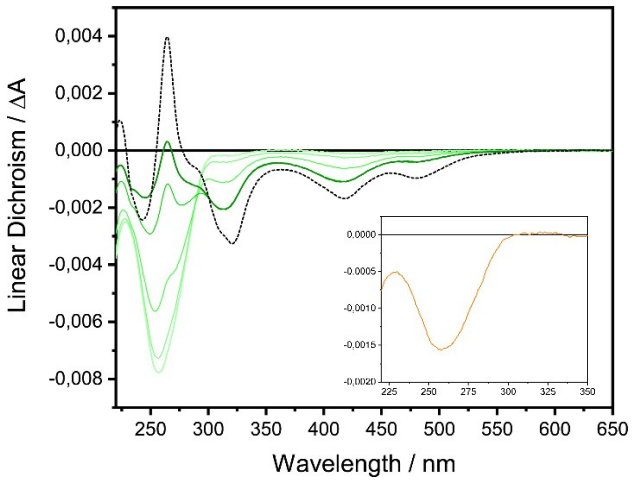

Figure 2. Linear dichroism spectra of Δ-**Ru-1** (green) and ΔΔ-**Ru-2** (dotted black, incubated 1 d at 50°C) in the presence of ctDNA at [base pairs]/[complex] ratio 5 in 50 mM NaCl aqueous buffer solution with 20% (w/w) PEG-400. The color change from light to dark specify spectral change for Δ-**Ru-1** with time (0.5 h, 1.5 h, 1 d, 2 d, and 7 d) after 50°C incubation. The concentration of ctDNA is 150 μM nucleotides. Inset shows the subtracted spectra of LD_{2d}-LD_{7d} for Δ-**Ru-1**.

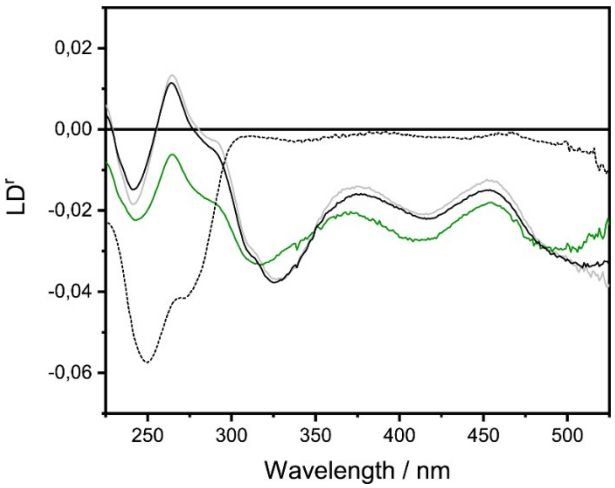

Figure 3. Reduced linear dichroism spectra of Δ-**Ru-1** and ΔΔ-**Ru-2** after incubation at 50°C in the presence of ctDNA at [base pairs]/[complex] ratio 5 in 50 mM NaCl aqueous buffer solution with either 0% or 20% (w/w) PEG-400 (black dotted: Δ, 0%; green: Δ, 20%; gray: ΔΔ, 0%; black solid: ΔΔ, 20%. The concentration of ctDNA is 150 μM nucleotides, and the time of incubation was 2 days for Δ-**Ru-1** and 1 day for ΔΔ-**Ru-2**.

View Article Online
DOI: 10.1039/D0CP00845A

pure DNA-signal without any complex contribution to a signal identical, albeit weaker, to the threaded ΔΔ-**Ru-2**.

As previously reported for the parent $[Ru(phen)_2dppz]^{2+}$ complex [2a,9a] and **Ru-2**[3d], **Ru-1** is quenched when free in aqueous solution but becomes brightly luminescent upon binding to DNA by intercalation, thus enabling observation of the intercalation process by monitoring the luminescence intensity change at 620 nm. Fig. 4 shows the kinetic traces obtained at 50°C for Δ- and Λ-**Ru-1** at different concentrations of PEG-400. In absence of PEG-400, only a slight immediate increase in luminescence is observed upon addition of ctDNA, but without any further increase in intensity even after several days. In a DNA solution containing PEG-400 a slow luminescence increase, indicative of intercalation of the bidppz moiety, is observed, and with increased PEG-400 concentration both the initial rate and the amplitude of this process increases. Since the plateau luminescence intensities for the two enantiomers of **Ru-2** are unaffected by the presence of PEG-400, we assume that also for **Ru-1** the quantum yield of intercalated complex is not affected significantly by the solvent composition. This suggest that the variation in luminescence intensity at the end of the initial phase of intercalation for **Ru-1** is due to a difference in concentration of intercalated **Ru-1** complexes, and that an increase in PEG-400 concentration not only speeds up the rate of threading but also shifts the equilibrium from an external non-luminescent binding mode to a binding mode that is intercalated and luminescent. At concentrations of PEG-400 of 20% and above, the logarithmic timescale reveals an extremely slow second phase of significant luminescence increase, that has not plateaued even after more than a week of incubation at 50°C.

Table 1 summarizes the association rate constants determined by fitting a biexponential model to the data (see ESI for fitting curves). The kinetic traces of ΔΔ- and ΛΛ-**Ru-2** in different PEG concentrations are presented in Fig. S4 in ESI. The first rate constant is assigned to the primary threading intercalation process.[12] Consistent for both **Ru-1** and **Ru-2** throughout the kinetic series is that the k_1 is larger for the Λ-enantiomers, indicating a faster threading for Λ- compared to Δ-enantiomers.[3d] The luminescence quantum yield for intercalated $[Ru(phen)_2dppz]^{2+}$ complexes is strongly increased by the presence of complexes intercalated into neighbouring basepair pockets[7], and the second rate constant for **Ru-2** has been assigned to a slow redistribution of the threaded complexes on the DNA lattice that increases the number of close neighbours.[13] A similar mechanism may be part of the explanation for the second, very slow phase of **Ru-1**.

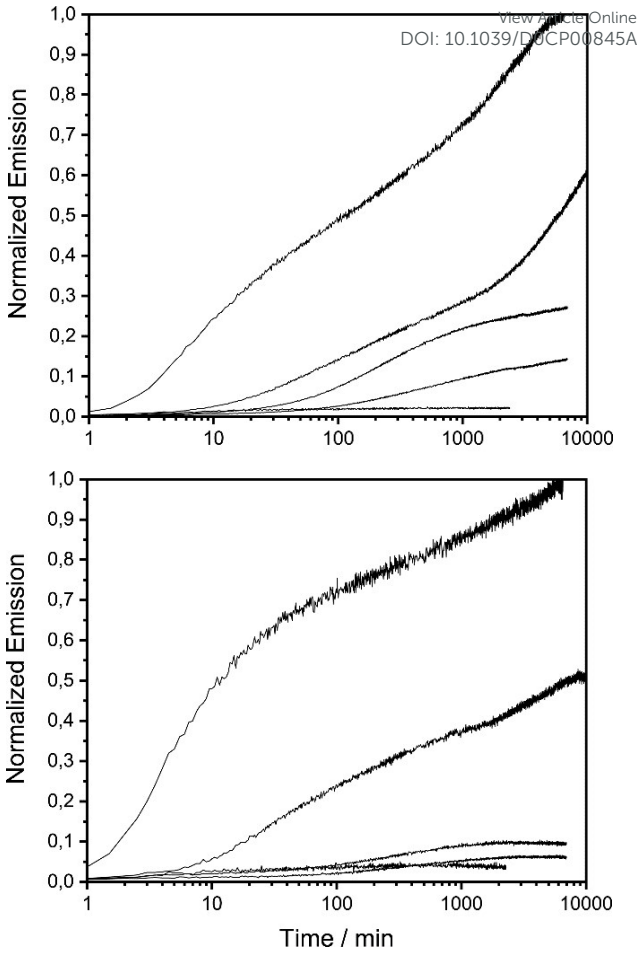

Figure 4. Association kinetics of Δ- (top) and Λ-**Ru-1** (bottom) in the presence of ctDNA, measured at different concentrations of PEG-400. PEG-400 concentrations from left to right are 40, 20, 15, 10 and 0% (w/w). Measurements performed at 50°C in 50 mM NaCl. The concentrations of complex and ctDNA were 15 μM and 150 μM nucleotides, respectively.

Table 1. Association rate constants and pre-exponential factors for threading intercalation into ctDNA.[a]

	ΔΔ		ΛΛ		Δ		Λ	
PEG-400 (%)	k_1*10^3/min^{-1} (α_1)	k_2*10^3/min^{-1} (α_2)	k_1*10^3/min^{-1} (α_1)	k_2*10^3/min^{-1} (α_2)	k_1*10^3/min^{-1} (α_1)	k_2*10^3/min^{-1} (α_2)	k_1*10^3/min^{-1} (α_1)	k_2*10^3/min^{-1} (α_2)
0	9.04 (0.70)	1.75 (0.30)	17.4 (0.61)	2.79 (0.39)	-	-	-	-
5	42.8 (0.73)	5.28 (0.27)	134 (0.76)	3.36 (0.24)	-	-	-	-
10	53.2 (0.75)	6.61 (0.25)	136 (0.80)	2.97 (0.20)	-	-	-	-
15	72.5 (0.77)	9.31 (0.23)	147 (0.86)	2.92 (0.14)	-	-	-	-
20	104 (0.81)	9.05 (0.19)	217 (0.87)	3.20 (0.13)	13.8 (0.29)	0.23 (0.71)	18.2 (0.59)	0.43 (0.41)
40	326 (0.91)	9.36 (0.09)	493 (0.87)	3.61 (0.13)	45.4 (0.49)	0.57 (0.51)	83.6 (0.73)	0.48 (0.27)

[a]Determined from luminescence kinetic traces obtained with 15 μM complex and 150 μM nucleotides in 50 mM NaCl after 50°C incubation.

View Article Online
DOI: 10.1039/D0CP00345A

Table 2. Luminescence decay parameters for **Ru-1** and **Ru-2** enantiomers in the presence of ctDNA and 20% (w/w) PEG-400.

Sample[a]	τ_1(ns)	α_1	τ_2(ns)	α_2	τ_{avg}[b] (ns)
Δ-**Ru-1**	75	0.53	475	0.47	263
Λ-**Ru-1**	47	0.42	177	0.58	122
ΔΔ-**Ru-2**	84	0.54	303	0.46	185
ΛΛ-**Ru-2**	59	0.81	231	0.18	92

[a]150 μM nucleotides and 15 μM complex in 50 mM NaCl after 50°C incubation.
[b]The average emission lifetime calculated as $\tau_{avg} = \alpha_1\tau_1 + \alpha_2\tau_2$.

Emission lifetime measurements were performed for both **Ru-1** and **Ru-2** in the presence of 20% PEG-400 and ctDNA, and the results are presented in Table 2. Two lifetimes were sufficient to fit the data for all samples (see ESI for fitting curves). As previously reported for **Ru-2**[3d], the Δ-enantiomer of binuclear **Ru-1** displays much longer lifetimes compared to the Λ-enantiomer. In addition, **Ru-2** is seemingly unaffected by the presence of PEG-400.

In a simple aqueous saline buffer solution the increased hydrophobicity of the bidppz ligand of **Ru-1** results in a higher prevalence of self-aggregation; a common occurrence with many Ru(II) polypyridyl complexes where two or more moieties spontaneously associates under equilibrium conditions.[14] Furthermore, the higher tendency for more hydrophobic Ru(II) complexes to self-aggregate has previously been demonstrated by our group by methyl substitution on the intercalative ligand.[15] With the addition of PEG-400 in the solvent, the PEG molecules, being hydrophobic, associate to the hydrophobic "tail" of **Ru-1**, preventing the assembling of aggregates.

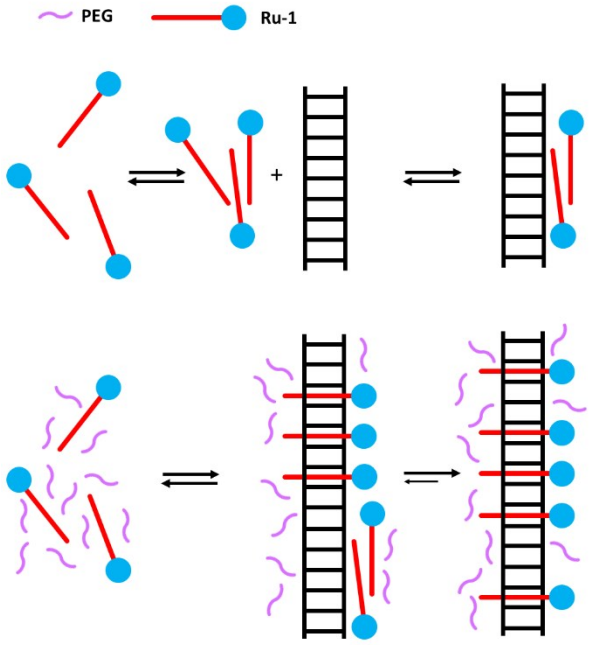

Figure 5. Binding model for **Ru-1** in the absence (top) and presence (bottom) of polyethylene glycol (PEG).

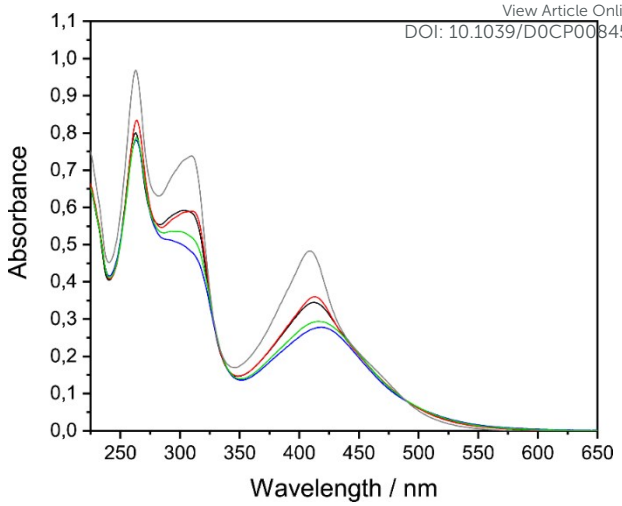

Figure 6. Absorption spectra of Δ-**Ru-1** (~10 μM) in different solvents: MeOH/H2O (1:1) (gray), 40% (w/w) PEG-400 + 50 mM NaCl buffer (red), MilliQ-pure water (black), 15% (w/w) PEG-400 + 50 mM NaCl buffer (green), 50 mM NaCl buffer (blue). All measurements were performed in room-temperature.

Our proposed binding model for **Ru-1** in the absence and presence of PEG-400 is presented in Fig. 5. To evaluate our hypothesis a series of absorption spectra were collected with stock solutions of Δ-**Ru-1** and ΔΔ-**Ru-2** in different solvents (MeOH/H_2O (1:1), H_2O, 50 mM NaCl buffer, 15% PEG-400 and 40% PEG-400). In the MeOH/H2O solvent, both complexes show very prominent absorption peaks at approximately 263 nm (mainly phenanthroline π→π* transitions), and at 311 nm (mainly biddpz π→π*) and 410 nm (bidppz π→π*, overlapping with the broad MLCT band). However, as shown in Fig. 6, by changing the solvent to pure water the intensity significantly drops for **Ru-1**, and the effects in the bidppz bands are even more prominent in a 50 mM NaCl buffer, indicating **Ru-1** to form aggregates in saline solution mainly through hydrophobic interactions of the bidppz ligands. By adding 40% PEG-400 in the saline buffer the absorption intensity is regained to a level close to pure water as solvent. Interestingly, the 15% PEG-400 and saline mixture appears to have very little effect on the observed hypochromicity of **Ru-1**, reflecting the weak emission increase in Fig. 4. As previously suggested, it appears that PEG-400 concentrations <20% are not sufficient to shift the equilibrium between aggregates and intercalated ligands. In contrast, the binuclear complex **Ru-2** shows significantly less hypochromicity in a saline solution (Fig S15 in ESI). Table S2 in ESI summarizes the maximum absorption peaks and hypochromicity of **Ru-1** and **Ru-2**.

Conclusions

In summary, by the addition of polyethylene glycol we have enabled threading intercalation of a novel ruthenium(II) complex, otherwise too hydrophobic to properly interact with the DNA polymer. The inclusion of the well-established **Ru-2** demonstrates that the presence of PEG-400 does not disrupt the final binding mode of the complex, but only accelerates the

View Article Online
DOI: 10.1039/D0CP00645A

initial intercalative binding process, thus enabling more efficient screening processes when characterizing new potential DNA binding drugs. For future investigation, in vivo bacterial studies of threading ruthenium complexes would be of great interest. In particular, the exploration of the bacterial cytosol to find whether its complex content could facilitate DNA interaction in means similar as observed here.

Conflicts of interest

There are no conflicts to declare.

Acknowledgements

The authors gratefully acknowledge the financial support from Kristina Stenborgs Stiftelse for Scientific Research (C 2018-2023), the Swedish Research Council (Vetenskapsrådet, 2016-05421) and the Chalmers Excellence Initiative Nano. BF also acknowledges support from the Ruth and Nils-Erik Stenbäck Foundation.

References

1 (a) M. R. Gill and J. A. Thomas, *Chem. Soc. Rev.*, 2012, **41**, 3179-3192; (b) A. Notaro and G. Gasser, *Chem. Soc. Rev.*, 2017, **46**, 7317-7337; (c) M. Pal, U. Nandi and D. Mukherjee, *Eur. J. Med. Chem.*, 2018, **150**, 419-445; (d) S. Thota, D. A. Rodrigues, D. C. Crans and E. J. Barreiro, *J. Med. Chem.*, **61**, 5805-5821; (e) V. Brabec and J. Kasparkova, *Coordin. Chem. Rev.*, 2018, **376**, 75-94.

2 (a) A. E. Friedman, J. C. Chambron, J. P. Sauvage, N. J. Turro and J. K. Barton, *J. Am. Chem. Soc.*, 1992, **112**, 4960-4962; (b) R. M. Hartshorn and J. K. Barton, *J. Am. Chem. Soc.*, 1992, **114**, 5919-5925; (c) Y. Jenkins, J. K. Barton, A. E. Friedman and N. J. Turro, *Biochemistry*, 1992, **31**, 10809-10816; (d) E. J. C. Olson, D. Hu, A. Hörmann, A. M. Jonkman, M. R. Arkin, E. D. A. Stemp, J. K. Barton and P. F. Barbara, *J. Am. Chem. Soc.*, 1997, **119**, 11458-11467; (e) R. B. Nair and C. J. Murphy, *J. Inorg. Biochem.*, 1998, **69**, 129-133.

3 (a) P. Lincoln and B. Nordén, *Chem. Comm.*, 1996, 2145-2146; (b) B. Önfelt, P, Lincoln and B. Nordén, *J. Am. Chem. Soc.*, 2001, **123**, 3630-3637; (c) L. M. Wilhelmsson, F. Westerlund, P. Lincoln and B. Nordén, *J. Am. Chem. Soc.*, 2002, **124**, 12092-12093; (d) J. Andersson, M. Li and P. Lincoln, *Chem.-Eur. J.*, 2010, **16**, 11037-11046; (e) J. Andersson and P. Lincoln, *J. Phys. Chem. B*, 2011, **115**, 14768-14775; (f) J. R. Johansson, Y. Wang, M. P. Eng, N. Kann, P. Lincoln and J. Andersson, *Chem.-Eur. J.*, 2013, **19**, 6246-6256; (g) A. A. Almaqwashi, J. Andersson, P. Lincoln, I. Rouzina, F. Westerlund and M. C. Williams, *Biophys. J.*, 2016, **110**, 1255-1263.

4 (a) L. Wu, A. Reymer, C. Persson, K. Kazimierczuk, T. Brown, P. Lincoln, B. Nordén and M. Billeter, *Chem.-Eur. J.*, 2013, **19**, 5401-5410; (b) A. A. Almaqwashi, T. Paramanathan, P. Lincoln, I. Rouzina, F. Westerlund and M. C. Wiiliams, *Nucleic Acids Res.*, 2014, **42**, 11634-11641; (c) D. R. Boer, L. Wu, P. Lincoln and M. Coll, *Angew. Chem. Int. Ed.*, 2014, **53**, 1949-1952; (d) M. Bahira, M. J. McCauley, A. A. Almaqwashi, P. Lincoln, F. Westerlund, I. Rouzina and M. C. Williams, *Nucleic Acids Res.*, 2015, **43**, 8856-8867.

5 (a) W. E. A. de Witte, M. Danhof, P. H. van der Graaf and E. C. M. de Lange, *Trends Pharmacol. Sci.*, 2016, **37**, 831-842; (b) G. Vauquelin, *B. J. Pharmacol.*, 2016, 2319-2334.

6 (a) A. K. Bilakhiya, B. Tyagi and P. Paul, *Inorg. Chem.*, 2002, **41**, 3830-3842; (b) Z. A. Siddique, K. Miyawaki and T. Ohno, *Croat. Chem. Acta*, 2008, **81**, 477-485; (c) X. L. Liang and L. F. Tan, *Aust. J. Chem.*, 2010, **63**, 1453-1461; (d) S. Ji, H. Guo, W. Wu, W. Wu and J. Zhao, *Angew. Chem. Int. Ed.*, 2011, **50**, 8283-8286.

7 (a) J. Andersson and P. Lincoln, *J. Phys. Chem B*, 2011, **115**, 14768-14775; (b) J. Andersson, L.H. Fornander, M. Abrahamsson, E. M. Tuite, P. Nordell and P. Lincoln, *Inorg. Chem.*, 2013, **52**, 1151-1159; (c) A. K. F. Mårtensson, M. Bergentall, V. Tremaroli and P. Lincoln, *Chirality*, 2016, **28**, 713-720; (d) A. K. F. Mårtensson and P. Lincoln, *Phys. Chem. Chem. Phys.*, 2018, **20**, 7920-7930; (e) A. K. F. Mårtensson, M. Abrahamsson, E. M. Tuite and P. Lincoln, *Inorg. Chem.*, 2019, **58**, 9452-9459.

8 B. Feng, R. P. Sosa, A. K. F. Mårtensson, K. Jiang, A. Tong, K. D. Dorfman, M. Takahashi, P. Lincoln, C. J. Bustamante, F. Westerlund and B. Nordén, *P. Natl. Acad. Sci. USA.*, 2019, **116**, 17169-17174.

9 (a) C. Hiort, P. Lincoln and B. Nordén, *J. Am. Chem. Soc.*, 1993, **155**, 3448-3454; (b) L. M. Wilhelmsson, E. K. Esbjörner, F. Westerlund, B. Nordén and P. Lincoln, *J. Phys. Chem. B*, 2003, **107**, 11784-11793.

10 (a) P. Lincoln and B. Nordén, *J. Phys. Chem. B*, 1998, **102**, 9583-9594; (b) T. Very, S. Despax, P. Hebraud, A. Monari and X. Assfeld, *Phys. Chem. Chem. Phys.*, 2012, **14**, 12496-12504.

11 (a) B. Nordén, M. Kubista and T. Kurucsev, *Q. Rev. Biophys.*, 1992, **25**, 51-170; (b) B. Nordén, A. Rodger and T. Dafforn, *Linear Dichroism and Circular Dicroism: A Textbook on Polarized-Light Spectroscopy*. Royal Sociaty of Chemistry: Cambridge, 2010; (c) A. Wada and S. Kozawa, *J. Polym. Sci. A*, 1964, **2**, 853-864; (d) M. Eriksson and B. Nordén, *Drug-Nucleic Acid Interactions*, 2001, **340**, 68-98.

12 P. Nordell and P. Lincoln, *J. Am. Chem. Soc.*, 2005, **127**, 9670-99671.

13 F. Westerlund, L. M. Wilhelmsson, B. Nordén and P. Lincoln, *J. Phys. Chem. B*, 2005, **109**, 21140-21144.

14 (a) R. Kaur and S.K. Mehta, *Coordin. Chem. Rev.*, 2014, **262**, 37-54; (b) L. Zeng, P. Gupta, Y. Chen, E. Wang, L. Ji, H. Chao and Z.-S. Chen, *Chem. Soc. Rev.*, 2017, **46**, 5771-5804.

15 A. K. F. Mårtensson and P. Lincoln, *Phys. Chem. Chem. Phys.*, 2018, **20**, 11336-11341.

View Article Online
DOI: 10.1039/D0CP00845A